Subterranean mMTC in Remote Areas: Underground-to-Satellite Connectivity Approach

Kaiqiang Lin, Muhammad Asad Ullah, Hirley Alves, Konstantin Mikhaylov, and Tong Hao

***Abstract*—Wireless underground sensor networks (WUSNs) promise to deliver substantial social and economic benefits across different verticals. However, many of the relevant application scenarios are located in remote areas with no supporting infrastructure available. To address this challenge, we conceptualize in this study the underground direct-to-satellite (U-DtS) connectivity approach, implying the reception of the signals sent by the underground massive machine-type communication (mMTC) sensors by the gateways operating on the low Earth orbit satellites. We start by discussing the two alternative architectures for enabling such networks and underline their features and limitations. Then, we employ simulations to model a smart-farming application scenario for studying the feasibility and performance of U-DtS mMTC based on LoRaWAN technology, with the focus on the effect of the parameters including the burial depths, soils characteristics, and communication settings. Our results reveal that the LoRa modulation fails to compete with the underground propagation losses and the high packets collision rate. However, the long range-frequency hopping spread spectrum (LR-FHSS) modulation is perspective for U-DtS networks and may enable connectivity for the subsurface nodes located at a depth of several dozens centimeters. Finally, we pinpoint the potential challenges and the research directions for future U-DtS studies.**

I. Introduction

Wireless underground sensor networks (WUSNs) *in-situ* monitor various subterranean entities through wirelessly connected underground sensors. Although the WUSNs do not require high data rates and can tolerate latency on data transmission, an energy-efficient communication is vital for the battery-powered underground sensors. Therefore, the low-power wide-area network (LPWAN) technology is favored for WUSNs. We recently investigated the possibility of underground-to-aboveground connectivity using LPWAN-grade massive machine-type communication (mMTC) wireless technologies [1], with the initial results highlighting that, the mMTC-based WUSNs can enable many applications, including but not limited to:

- **Smart agriculture:** Tackling the global food demand expected to double by 2050, the 5G innovation verticals promote smart farming to collect accurate information from sensors for timely decision-making, precise remote operation and minimizing maintenance costs. The WUSNs for smart farming and irrigation monitoring system promise gain in crop yield in the remote areas which lack water resources and labour.
- **Underground pipelines monitoring:** Underground pipelines serve as lifelines of modern civilization by supplying water, natural gas, and crude oil over hundreds to thousands of kilometres. Frequent large pipeline incidents bring significant economic costs, severe environmental pollution, and casualties [2]. It is very challenging to detect the potential risks of pipelines in remote or rural areas, whereas mMTC-based WUSNs may provide technological assistance by, for instance, realizing the real-time leakage detection and the localization of fragile underground pipeline sections.
- **Disaster rescue operations:** Positioning systems are critical for increasingly frequent rescue operations for natural disasters, e.g., earthquake and landslide. However, existing positioning operations still largely rely on conventional geophysical techniques, which leads to low rescue efficiency. The mMTC-based WUSNs enables real-time geological monitoring and accurate positioning of the trapped people and goods in hazard zones.

Notably, many of these applications imply operations in remote areas, where the availability of communication infrastructure cannot be guaranteed. Due to scarce network resources, severe attenuation in underground soils and economic reasons, mMTC-based WUSNs cannot offer large-scale underground monitoring in hard-to-reach or disaster rescue areas. Motivated by this, we explore the feasibility of underground LPWAN sensors and low Earth orbit (LEO) satellites integration, implying underground-to-satellite (UtS) networks.

The main contributions of this work are as follows:

1) We propose and analyze two alternative communication architectures for the mMTC-based direct and indirect UtS networks depicted in Fig. 1 and discuss their pros, cons, and relevant trade-offs.
2) We discuss and characterize the suitability of LoRaWAN LPWAN technology for the underground direct-to-satellite (U-DtS) connectivity approach, in which, we carefully analyze two modulation-coding schemes (MCSs) of LoRaWAN, i.e., LoRa and LoRa-frequency hopping spread spectrum (LR-FHSS).
3) Finally, we develop the simulator which features real-life parameters with (i) the position of center-pivot

K. Lin and T. Hao are with the College of Surveying and Geo-Informatics, Tongji University, Shanghai, China. E-mail: lkq1220@tongji.edu.cn; tonghao@tongji.edu.cn. (*Corresponding Author: T. Hao*)

M. Asad Ullah, H. Alves and K. Mikhaylov are with the Centre for Wireless Communications (CWC), University of Oulu (UO), Finland. Email: Muhammad.AsadUllah@oulu.fi; Hirley.Alves@oulu.fi; konstantin.mikhaylov@oulu.fi.

This work was supported in part by National Key Research and Development Program of China (No. 2021YFB3900105), National Natural Science Foundation of China (No. 42074179 and 42211530077), the Academy of Finland, 6G Flagship program (No. 346208), and the China Scholarship Council.

irrigation fields in the farm; (ii) accurate path loss model which accounts for the absorption in soils; and (iii) time-varying characteristics of the fading effect due to satellite mobility. By comparing two MCSs, the results reveal that LR-FHSS can achieve reliable connectivity between massive underground sensors and the satellite with higher robustness against the co-channel interference compared to LoRa. Meanwhile, the interplay between packet delivery, energy efficiency, and soil characteristics is highlighted to inspire further studies and experiments in this new research direction.

II. Technical Background and Recent Development

A. WUSNs and LPWAN-grade mMTC Technologies

Generally, two main networking approaches are adopted in WUSNs - one is based on ad-hoc networks and the other is based on centralized networks (i.e., through gateways (GWs)) [3]. In ad-hoc networks, data transmission between buried nodes can be established through multi-hops configuration. However, the practical communication distance between underground nodes is limited to 12 m [4], which largely limits the implementation of ad-hoc networks for large-scale underground monitoring applications. The centralized networks, on the other hand, allow direct links between underground nodes and GWs, thus reducing underground routing steps that are normally power intensive. Therefore, from the perspective of reliable connectivity and energy efficiency, the centralized networks, e.g., LPWAN, are preferred for WUSNs.

Currently, LoRaWAN, NB-IoT, and Sigfox are three technologies leading in the LPWAN market. Among them, NB-IoT and Sigfox are deployed by dedicated mobile network operators (MNOs), thus their availability can be limited or often infeasible for remote area applications. LoRaWAN, however, can be deployed by either MNOs or microoperators, which enables implementation flexibility for WUSNs in remote areas.

Notably, previous studies have experimentally investigated the potential of LoRa modulation, underlying LoRaWAN, for WUSNs. The results show that the underground-to-aboveground connectivity for a LoRaWAN device operating the LoRa MCS fails to reach 100 m at the burial depth of 0.4 m [1]. Herein, the key transmission obstacle is the substantial losses in the subterranean wireless channel, which is largely affected by soil properties (e.g., texture and bulk density), volumetric water content (VWC), burial depth, and nodes' operating frequency, etc. For qualifying communication of underground mMTC in remote areas, since a dense deployment of GWs is economically infeasible, one possible solution is to increase the coverage of the GW by deploying it on the satellite, i.e., DtS.

B. Satellite Systems and mMTC DtS Connectivity

According to the Union of Concerned Scientists, there are about 5,465 operating satellites in orbit as of May 1, 2022, of which 4,700 are in LEO. In addition, over 100,000 satellites are expected to encircle the Earth over the next 10 years. Note that LEO satellites feature the lowest launch cost, signal attenuation and propagation delay which ranges from 2 ms to 10 ms, with a caveat of smaller coverage and higher Doppler. Therefore, a constellation comprising tens of satellites is required for enabling global seamless connectivity, e.g., Telesat.

Over the years, various connectivity services have been enabled by the satellites: telephony, navigation, Internet connectivity, etc. Following this trend, the integration of satellite systems with LPWAN-grade mMTC technologies has been conceptualized [5]. To this end, Lacuna Space and Semtech reported successful experimental trials of LoRaWAN DtS connectivity between a ground node and an LEO satellite implying LoRa MCS [6]. To tackle the connectivity challenges in remote areas, recent studies investigated the feasibility and efficiency of mMTC DtS networks [5]–[7].

Specifically, [5] and [6] demonstrate that a LoRa packet could reach the LEO satellite even at the largest distance around 2300 km with over 97% success probability. Notably, they conclude that the primary reason behind the degradation of the overall packet delivery success probability is co-channel interference due to simultaneous transmissions from other nodes in the same channel. To further increase the reliability of conventional LoRa, in November 2020, LR-FHSS MCS was introduced into the LoRaWAN protocol, which supports up to eleven million uplink packets daily. In [7], an initial scalability analysis of LR-FHSS DtS connectivity illustrates that this new modulation substantially outperforms conventional LoRa and can support a large-scale non-terrestrial network (NTN).

C. LoRaWAN MCSs: LoRa and LR-FHSS

1) LoRa: It is a derivative of chirp spread spectrum MCS in LoRaWAN. LoRa offers levels of freedom in the physical layer, i.e., bandwidth (BW), code rate (CR), and spread factor (SF) to leverage the quasi-orthogonality of transmissions. By varying physical layer parameters, different trade-offs between radio coverage and energy consumption can be achieved. Despite the wide adoption of LoRa MCS in LoRaWAN, the network capacity and collision robustness are limited by Aloha-like media access protocol.

2) LR-FHSS: Compared with LoRa, LR-FHSS is only used for uplink communication currently, it improves the reliability and robustness to the interference to support large-scale mMTC through the following three operations.

1) Link budget. In the Federal Communications Commission (FCC) region, LR-FHSS offers at least 13 dB more link budget compared to LoRa MCS for covering remote applications.
2) Frequency hopping. For the uplink communication process, an LR-FHSS device sends each packet fragment (i.e., the header or a data fragment) on another randomly-picked frequency channel. Herein, in a single operating channel width (OCW) channel, LR-FHSS specifications define 3120 occupied bandwidth (OBW) physical carries (with a bandwidth of 488 Hz) for the new data rates (DRs), i.e., DR5 and DR6 in the FCC region. On the contrary, LoRa carries a complete transmission in a single channel which causes higher probability of co-channel interference.

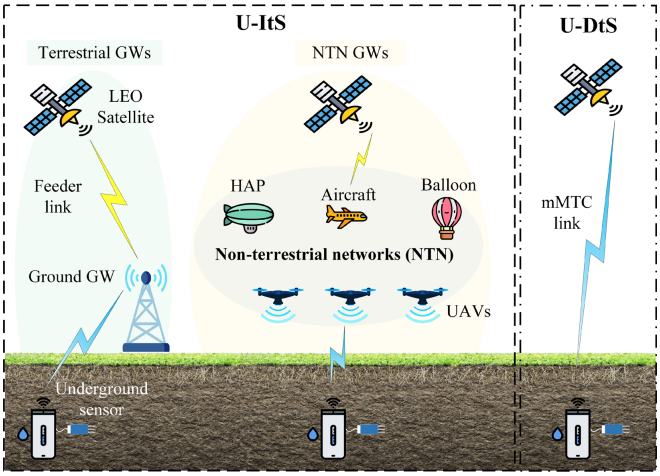

Fig. 1. U-ItS and U-DtS implementation topologies to enable WUSNs in remote areas, where U-ItS has two different deployment scenarios for terrestrial and non-terrestrial GWs.

3) Redundancy and coding. Unlike LoRa, an LR-FHSS device first transmits $\bar{N} = 1 \ldots 4$ replicas of a 233.472 ms-duration header by randomly selecting the carrier frequency. Then, the MAC payload and cyclic redundancy check are encoded and cut into small fragments no longer than 102.4 ms before being sent sequentially through a randomly selected OBW channel for each fragment. Therefore, a successful LR-FHSS packet reception at the GW needs to satisfy two conditions: (1) at least one header is received, and (2) the number of received fragments exceeds the reception threshold which is dependent on the CR [7].

Despite the major technical progress of mMTC and DtS connectivity, it remains unclear whether introduction of a subterranean communication channel component, which is characterized by a much higher attenuation than the on-air channel, would allow U-DtS connectivity and, if yes, under which conditions. To answer this question, in the next section we first discuss the different network architectures and configuration options for UtS connectivity and then generate numeric results to evaluate its feasibility.

III. UtS Network Architectures

A. Underground Indirect-to-Satellite (U-ItS)

The U-ItS architecture can be subdivided into:

1) U-ItS with terrestrial GW: This hybrid indirect network architecture comprises underground, ground and satellite segments. Specifically, underground devices transmit the monitored data to ground GWs through mMTC technologies. Next, the terrestrial GWs stream the acquired data further to the satellite over the feeder link, which requires expensive hardware and monthly liability for the satellite data plans. The main advantage is that this communication architecture relies on mature and proven technologies and products. Furthermore, it allows the data from underground devices to be aggregated and compressed before streaming to an LEO satellite, thus effectively reduces traffic loads and overheads. This approach's downside is the pricey deployment of more complicated terrestrial network infrastructures, which can also be fragile for some underground applications, e.g, disaster rescues.

2) U-ItS with non-terrestrial (NT) GW: We can also consider an NT topology, i.e., a GW deployed on an aerial platform e.g., unmanned aerial vehicles (UAVs) or high altitude platforms (HAPs). These NT GWs backhaul the buried sensors data to the satellite over the feeder link. Unlike the terrestrial GW, the mMTC GW on UAVs or HAPs can offer easy, on-demand, and quick wireless radio access to underground mMTC sensors in disaster-stricken or remote areas. However, due to UAVs' weather sensitivity, limited coverage, and short flight window, this NT strategy may not be suitable for scenarios which requires all-weather, 24/7 and seamless connectivity.

B. Underground Direct-to-Satellite (U-DtS)

This alternative architecture promises direct mMTC wireless connection between buried sensors and an NT GW deployed at a satellite without any mediator, e.g., local GW and aerial modem, which significantly simplifies the network topology.

Nonetheless, there are several concerns and challenges associated with U-DtS connectivity. The first one is the network scalability issue. Note that a radio receiver of a satellite has to handle myriads of small data produced by massive underground sensors, which leads to a high interference and packets collision. Second, strong radio frequency attenuation in soils and hundreds to thousands of kilometers distance between sensors and a satellite result in high path loss, which need to be countered by high transmit power of nodes. Notably, the attenuation caused by ionosphere, atmospheric gases, fog, clouds and rain droplets for the conventional mMTC technologies working in sub-GHz frequency bands can be negligible [8]. Finally, the mobility of satellite and dynamic underground environments owing to precipitation will fluctuate the radio channel resulting in complications for MCSs, which will negatively impact packet delivery rate and energy efficiency.

IV. U-DtS System over LoRaWAN: Proof of Concept for Remote Farming Case

The underground LPWAN applications have already been investigated in the literature (e.g., [1], [9]), making it a ready jigsaw in both U-ItS and U-DtS. Notably, by increasing the density of the terrestrial GWs in U-ItS, both the propagation and the scalability challenges can be addressed, however, it is economically insufficient, and even impractical for remote areas. Therefore, we focus on the more affordable and challenging topology, i.e., U-DtS, to assess its feasibility with the difficult underground communication channel conditions. Note that, to gain in-depth insight into this approach's feasibility, reliability, and trade-offs, we narrow down our work to LoRaWAN technology, which features two MCSs, i.e., LoRa and LR-FHSS. Figure 2 (a) and (b) illustrates the simulation scenario and target application, respectively. The corresponding key parameters and those of LoRaWAN MCSs are listed in Table I.

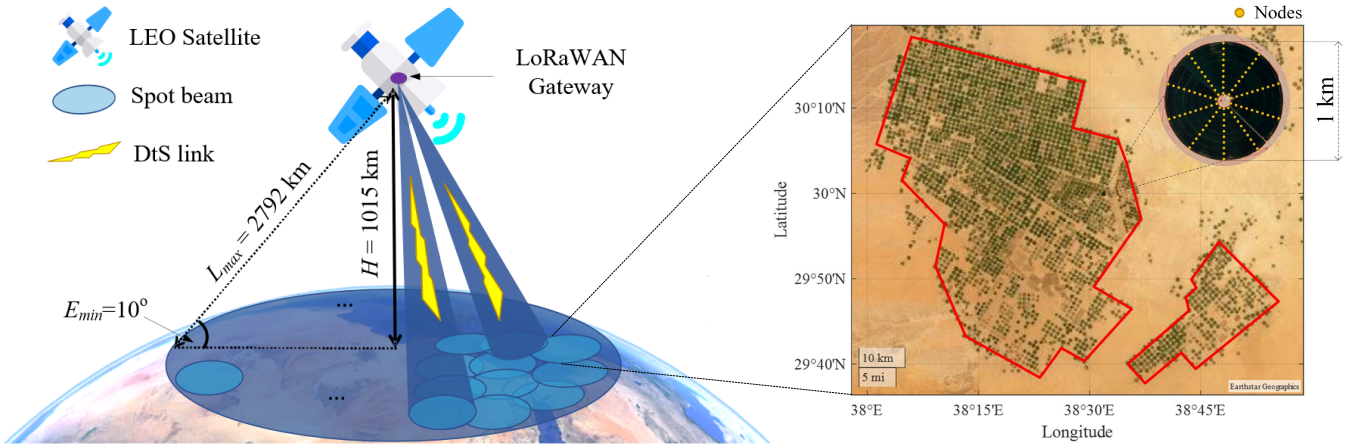

(a) Simulated scenario and key notations (b) Al Jouf Arable farm

Fig. 2. Simulated smart farming scenario, where (a) exhibits the architecture of the U-DtS approach with key notations and (b) illustrates the geographical location of the simulated center-pivot irrigation farm marked by red lines.

TABLE I
SYSTEM MODEL AND PARAMETERS FOR MONTE CARLO SIMULATIONS

Parameters	**Values**
Operation Environments [10]	
No. of field circle (M)	3045
Nodes/field circle (S)	100
Total nodes (N)	304,500
Node deployment	Equidistant
Burial depth (D)	*var* (0.35 m by default)
Volumetric water content (VWC)	11.19% (*in-situ*), 30%
Clay (C)	16.86% (*in-situ*), 50%
PHY payload (PL)	10 Bytes
Report period (T)	1800 s
Traffic pattern	Periodic
Telesat-like Satellite Configuration	
Elevation angles (E)	$10° \leq E \leq 90°$
Rician factor (K)	$1.24 \leq K \leq 25.11$
Orbital height (H)	1015 km
Link distance (L)	1015 km∼2792 km
Radio Configuration	
Carrier frequency (f_c)	915 MHz
Antenna gains	G_t=2.15 dBi, G_r=35 dBi
Path loss exponent (η)	2
SIR threshold (γ)	6 dB
LoRa MCS [7], [11]	
Transmit power (P_{tx})	20 dBm
Transmit current (I_{tx})	133 mA
SF	10
LoRa BW	125 KHz
Frequency channels	64
LoRa receiver sensitivity (SF10)	-132 dBm
LR-FHSS MCS [7], [11]	
Transmit power (P_{tx})	28 dBm
Transmit current (I_{tx})	650 mA
DR5/DR6 OBW channels	3120
Header replicas ($\bar{N}$)	3 (DR5), 2 (DR6)
CR	$\frac{1}{3}$ (DR5), $\frac{2}{3}$ (DR6)
Header replica duration (T_H)	233.472 ms
Fragment duration (T_F)	102.4 ms
LR-FHSS OBW bandwidth	488 Hz
LR-FHSS receiver sensitivity	-137 dBm

A. Simulation Parameters and Configurations

To investigate the feasibility of U-DtS connectivity, we select the real-life center-pivot irrigation farm (named Al Jouf Arable farm) with a total of M=3045 irrigation circle fields in northern Saudi Arabia, as illustrated in the right panel of Fig. 2 (b). We numerically imply that S=100 underground devices are equidistantly buried in each irrigation circle at a depth of 0.35 m to avoid the effects of mechanical farming activities and to efficiently monitor the soil conditions [12], while each node transmits a 10-Byte uplink packet with a period of T=1800 s. We set the real-life soil characteristics, e.g., VWC and clay percentage of the selected farms to capture the real underground path loss [10]. In such underground deployment, we imply each LoRaWAN node is equipped with a 2.15 dBi-gain omnidirectional antenna. Next, we envision a LoRaWAN NT GW deployed on a Telesat-like satellite which provides multiple spot beams with the high antenna gain of 35 dBi. Herein, we imply a total of N=304,500 sensors, spreading across the whole farm, are covered by one spot beam. Furthermore, we consider the dynamic evaluation angle ($10° \leq E \leq 90°$) that leads to the variation of channel characteristics modeled by the Rician-fading channel model with the Rician factor (K), and the communication distance from 2792 km to 1015 km between an underground node and the satellite-based GW.

We consider U-DtS system operating in the US 915 MHz ISM band with the transmit power of 20 dBm for LoRa and 28 dBm for LR-FHSS in the FCC region [11]. For LoRa's configurations, the DR0 featuring the strongest propagation capability (which corresponds to SF10, BW125, the receiver sensitivity of -132 dBm and a maximum of 64 uplink channels) is implied to overcome strong signal attenuation in soils. Note that LR-FHSS modulation can coexist with the conventional LoRa without redesigning the legacy LoRaWAN network architecture and protocol [7]. In the FCC region, only DR5 and DR6 support LR-FHSS. Both DRs allow a device to leverage an OCW channel comprising 3120 OBW channels. Furthermore, DR5 implies a slower bit rate (162 bits/s) with a CR of $\frac{1}{3}$ and header repetitions of $\bar{N}$=3, while DR6 has a higher bit rate of 325 bits/s by using CR=$\frac{2}{3}$ and $\bar{N}$=2. Thanks to the larger allowed transmit power and the higher receiver sensitivity (-137 dBm), the maximum link budget of LR-FHSS

achieves 167 dB, which is 13 dB greater than that of LoRa SF10 [11].

To offer more accurate insights into the feasibility and potential trade-offs associated with two MCSs in the U-DtS connectivity approach, we developed the MATLAB-based Monte Carlo U-DtS simulator based on the LR-FHSS model proposed in [7]. Our simulator models the real-life remote irrigation scenario, and uses accurate U-DtS attenuation model and energy consumption model. The total path loss accounts for (i) the absorption in soils calculated by the modified Friis model based on the mineralogy-based soil dielectric model introduced in [1], [9] and (ii) free-space path loss for line-of-sight signal propagation by considering the mobility of satellite characterized by the Rician factor (K). The probability of a packet being correctly received by a LoRaWAN GW is denoted as success probability (P_S), comprising two components. The former one, P_{SNR}, represents the probability of signal-to-noise ratio (SNR) for the received packet exceeding the DRs-specific SNR demodulation threshold (D_{SNR}=-15 dB for LoRa DR0 and D_{SNR}=4 dB for GMSK in LR-FHSS DR5/DR6) [7], [11]. The latter one, P_{SIR}, considers the interfering signals and denotes the possibility of the packets being correctly demodulated by leveraging the capture effect. To benefit from the capture effect, the signal-to-interference ratio (SIR) of the target packet should be above a certain threshold (γ=6 dB).

Furthermore, the energy per packet (EPP) denotes as the average amount of energy consumed by an end-device to deliver a packet to the satellite GW, which is calculated to assess the energy consumed for a packet successfully received by the satellite GW, thus to reveal the potential battery lifetime of each underground node. To accurately model the battery lifetime, we implement the complete LoRaWAN Class A end-devices energy consumption model (including the waking up and going back to sleep states) based on [13, eq. (2)] and assume that the battery capacity of each underground device is 3000 mAh. Herein, the values of operating voltage and transmit current are obtained from the datasheets of SX1262 module.

B. Selected Numeric Results

Firstly, we analyze the feasibility of an uplink signal from an underground node reaching a satellite-based GW. Figure 3 illustrates the effects of node's burial depth and soil properties, i.e., VWC and clay percentage, on the received power at the GW. Moreover, it also depicts the receiver's sensitivity thresholds for LoRa and LR-FHSS to illustrate the minimum power levels at which GW can receive the packet. Note that, for a fair comparison of the two MCSs in Fig. 3, the same transmit power (i.e., P_{tx}=20 dBm) is used. The attenuation in soils is an essential component for the total path loss in the U-DtS connectivity, thus we plot it separately in the four topmost solid lines in Fig. 3. One can see that the received power degrades significantly with a larger burial depth of the node. From the perspective of the soil characteristics, VWC of soils has a stronger effect on the signal attenuation compared with the soil composition, especially at higher clay

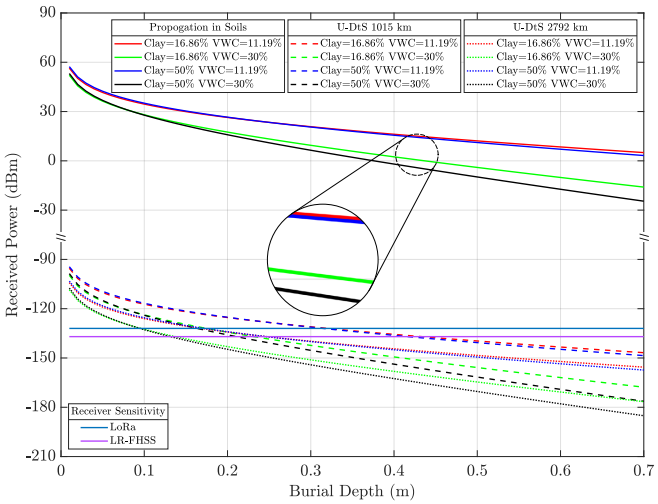

Fig. 3. The power of the received signal as a function of LoRaWAN node's burial depth, clay percentage and VWC. The top four solid lines represent the received power within the underground environment (from the buried node to the ground surface), where the dashed and dotted lines denote the received power at the minimum and maximum possible distance at 1015 km and 2792 km, respectively. The bottom solid lines depict the receiver sensitivity threshold for LoRa and LR-FHSS, respectively.

percentage. If the burial depth is higher than 0.2 m, the received power for VWC=30% at the distance of 1015 km is even lower than that for VWC=11.19% at the maximum distance of 2792 km. On the other hand, for the *in-situ* case of VWC=11.19%, clay=16.86% and the distance to a satellite is 1015 km, the received power is below the receiver sensitivity of LoRa for node's depth of 0.33 m. At the same time, if using LR-FHSS MCS, the received signal stays above the receiver sensitivity when the burial depth reaches 0.43 m. Notably, a node operating LR-FHSS can use up to P_{tx}=28 dBm in the FCC region [11] (compared to the maximum 20 dBm for LoRa), which indicates that LR-FHSS can establish the U-DtS connectivity at larger depths compared to LoRa.

The success probability P_S and its components (i.e., P_{SNR} and P_{SIR}) for two MCSs of LoRaWAN as a function of the distance from the nodes to the satellite are depicted in Fig. 4, with the time-varying characteristics of dynamic Rician factor (K). Note that Figs. 4 and 5, we imply that the nodes are buried at the depth of 0.35 m with *in-situ* VWC=11.19% and clay=16.86%, as well as P_{tx}=28 dBm for LR-FHSS.

In Fig. 4, the P_{SNR} curve ($<$0.03) for LoRa reveals that it cannot establish the connectivity between the underground sensors and the satellite regardless of the distance between the two. However, the P_{SNR} of LR-FHSS remains above 0.9 up to 1900 km, after which P_{SNR} drops to 0.624 at the maximum coverage distance of 2792 km. Note that the P_{SIR} for DR0 remains around 0.22 for all distances due to the high co-channel interference caused by myriads of uplink packets. Meanwhile, both DR5 and DR6 demonstrate a higher P_{SIR} of over 0.95 because LR-FHSS exploits frequency hopping and efficiently reduces the chances of collisions through increasing the number of physical channels ($\sim$3120 OBW channels) and redundant physical headers and lowering CR. More specifically, the P_{SIR} of DR5 is 0.038 higher than that of DR6 owing

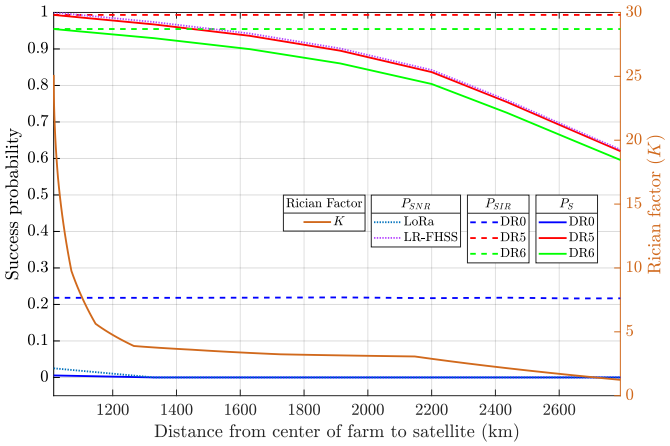

Fig. 4. The average success probability P_S as a function of distance from the farm center to a satellite and its components: the probability of SNR at a LoRaWAN GW exceeding the demodulation threshold P_{SNR} and the probability P_{SIR} of interference not blocking the reception of a packet. The right y axis illustrates the variation of the channel characteristics (the Rician factor (K)) with the distance.

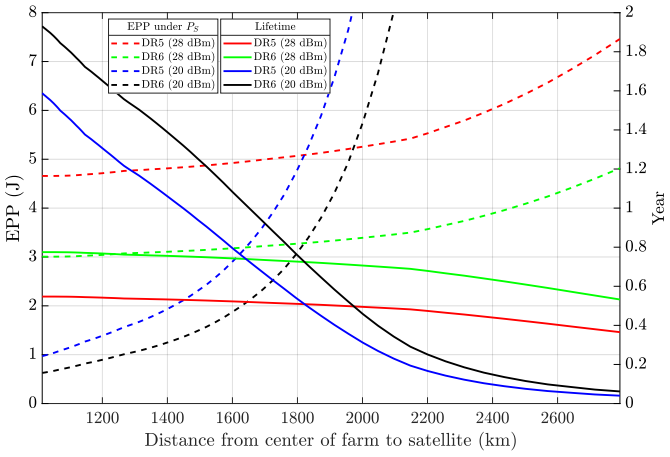

Fig. 5. The EPP for LR-FHSS and the lifetime of an underground device operating with DR5 and DR6 under two transmit power (i.e., 20 dBm and 28 dBm) as a function of the communication distance.

to the lower CR of $\frac{1}{3}$ and higher header replicas $\bar{N} = 3$. The overall success probability P_S of DR0 approximately retains 0 for all distances, while DR5 stays above 0.620 at the maximum distance, slightly better than DR6.

We also compare the EPP and lifetime of each underground device under both LR-FHSS DRs and two transmit powers (i.e., 20 dBm and 28 dBm), as shown in Fig. 5. Note that due to the high success probability (i.e., $P_S \geq 80\%$), the lifetime of DR5 and DR6 under P_{tx}=28 dBm tardily declines before the distance is 2200 km, compared to that under P_{tx}=20 dBm. Figure 5 reveals that the EPP for DR6 is significantly better than that of DR5; this is because although DR5 shows the better success probability, the time-on-air of DR5 (1423.69 millisecond) is much higher than that of DR6 (883.02 millisecond), which is the determinant factor in this case. More specifically, within the communication distance of 1830 km for both DR5 and DR6, the EPP with P_{tx}=20 dBm is smaller than that with P_{tx}=28 dBm, owing to the lower transmit current. Figure 5 also reveals that an underground device configured with DR6 and P_{tx}=28 dBm has the operation lifetime of at least 0.53 years under the relatively high transmission frequency, i.e., 30 min. The battery lifetime can be further improved by adjusting reporting period, according to the requirement of U-DtS system. For instance, increasing reporting period will improve P_{SIR} (owing to lower traffic load) and reduce the total energy consumption, which prolongs the battery lifetime.

V. Challenges and Further Research Directions

The above quantitative analysis verifies the feasibility and scalability of U-DtS connectivity approach, and that its performance is significantly affected by the complex subterranean environments, as well as the communication distance between the sensors and the satellite. The balance between the success probability and energy efficiency can be adjusted by different DRs. Notably, the investigated U-DtS approach can be further generalized for other underground scenarios, such as underground pipeline monitoring and disaster rescue operations. However, some open issues should still be carefully addressed when merging mMTC and WUSNs for U-DtS connectivity, as summarized below:

- **Surface shadowing and interference:** As U-DtS connectivity is affected by different seasonal crops or other weather conditions (e.g., snow cover), further studies and, especially, field experiments are needed to investigate the impact of the shadowing surfaces on the success probability. In our study, we implied the interference only from the LoRaWAN devices buried in the simulated farm. The interference effects coming from other devices working in the same frequency bands on the U-DtS connectivity shall be investigated in future work.
- **Intelligent ADR:** As shown by the previous studies, the adaptive DR (ADR) mechanism allows the fine-tuning of the performance of LoRaWAN. Our results illustratively show that the signal attenuation in U-DtS connectivity varies with soils' properties, which shall be considered in ADR. This calls for the development of the novel ADR schemes to intelligently optimize the DR that enables the energy-efficient connectivity in dynamic underground environments.
- **Network lifetime:** Energy efficiency is especially crucial for WUSNs. Besides energy-consumption optimization mechanisms for traffic pattern and communication parameters such as transmit power and ADR, the energy budget can be boosted through energy-harvesting technologies, e.g., wireless energy transfer, ambient back-scattering, and vibration energy harvesting. The efficiency optimization under energy harvesting constraints represents an interesting research direction to explore.
- **Frequency regulatory compliance:** It is known that the LoRaWAN follows regional frequency plans and regulations. It is worth investigating how the U-DtS systems performance varies with regions (e.g., Europe and Asia).
- **Enabling downlink communication:** Note that LoRaWAN only supports LR-FHSS in uplink, that is why

the conventional LoRa is required for downlink. However, our results reveal that the LoRa modulation is incompetent for the U-DtS connectivity due to the stronger path loss in soils. To allow the downlink, higher transmit power, larger antenna gains and optimal carrier frequency are needed to compete against the subterranean path loss. Furthermore, due to the mobility of satellites and strict duration for LoRaWAN receive windows, the establishment of the downlink communication will be a critical challenge for U-DtS.

VI. Conclusion

To extend the recently emerged DtS mMTC to the subterranean domain, in this article, we propose the underground DtS (U-DtS) to merge the WUSNs and DtS mMTC. After discussing the direct and indirect architectures, we focus on assessing the feasibility of U-DtS. Through extensive modelling of a realistic farming scenario via two MCSs of LoRaWAN (LoRa and LR-FHSS), our numeric results demonstrate that LR-FHSS achieves reliable connectivity between an underground device at a depth of some dozens of centimetres and a satellite with significant interference rejection. On the other hand, the conventional LoRa MCS underperforms due to the limitation of the link budget, the high packet collision probability, and the strong attenuation in a complex underground environment. Our results also indicate the effect of the soil conditions (e.g., VWC and clay percentage) on the communication channel and the overall performance of the proposed U-DtS approach. We believe that our work which establishes the baseline and confirms the potential feasibility of LoRaWAN U-DtS, will motivate future modeling and experimentation to take this novel concept further. Finally, we consider investigating system cost optimization, Doppler shift and proof-of-concept experiments for U-DtS worth looking at.

References

[1] K. Lin *et al.*, "Experimental Link Quality Analysis for LoRa-Based Wireless Underground Sensor Networks," *IEEE Internet of Things J.*, vol. 8, no. 8, pp. 6565–6577, 2021.

[2] Statista, "Total costs of reported oil and gas pipeline incidents in the United States from 2001 to 2020," Accessed: Sep. 1, 2022. [Online]. Available: https://www.statista.com/statistics/1271665/us-pipeline-incidents/

[3] I. F. Akyildiz *et al.*, "Wireless underground sensor networks: Research challenges," *Ad Hoc Networks*, vol. 4, no. 6, pp. 669–686, 2006.

[4] M. C. Vuran *et al.*, "Internet of underground things in precision agriculture: Architecture and technology aspects," *Ad Hoc Networks*, vol. 81, pp. 160–173, 2018.

[5] M. Asad Ullah *et al.*, "Massive Machine-Type Communication and Satellite Integration for Remote Areas," *IEEE Wireless Communications*, vol. 28, no. 4, pp. 74–80, 2021.

[6] M. Asad Ullah *et al.*, "Enabling mMTC in Remote Areas: LoRaWAN and LEO Satellite Integration for Offshore Wind Farm Monitoring," *IEEE Trans. Ind. Informat.*, vol. 18, no. 6, pp. 3744–3753, 2022.

[7] M. Asad Ullah *et al.*, "Analysis and Simulation of LoRaWAN LR-FHSS for Direct-to-Satellite Scenario," *IEEE Wireless Commun. Lett*, vol. 11, no. 3, pp. 548–552, 2022.

[8] A. Al-Hourani *et al.*, "On Modeling Satellite-to-Ground Path-Loss in Urban Environments," *IEEE Commun. Lett.*, vol. 25, no. 3, pp. 696–700, 2021.

[9] D. Wohwe Sambo *et al.*, "Wireless Underground Sensor Networks Path Loss Model for Precision Agriculture (WUSN-PLM)," *IEEE Sensors J.*, vol. 20, no. 10, pp. 5298–5313, 2020.

[10] Y. A. Al-Rumikhani, "Effect of crop sequence, soil sample location and depth on soil water holding capacity under center pivot irrigation," *Agricultural Water Management*, vol. 55, no. 2, pp. 93–104, 2002.

[11] Semtech, "AN1200.64 LR-FHSS System Performance," 2022, Accessed: Sep. 1, 2022. [Online]. Available: https://www.semtech.com/products/wireless-rf/lora-edge/lr1120

[12] X. Dong *et al.*, "Autonomous precision agriculture through integration of wireless underground sensor networks with center pivot irrigation systems," *Ad Hoc Networks*, vol. 11, no. 7, pp. 1975–1987, 2013.

[13] R. M. Sandoval *et al.*, "Deriving and Updating Optimal Transmission Configurations for Lora Networks," *IEEE Access*, vol. 8, pp. 38 586–38 595, 2020.

Biographies

Kaiqiang Lin (S'19) is currently pursuing the Ph.D. degree at the College of Surveying and Geo-Informatics, Tongji University, Shanghai, China.

Muhammad Asad Ullah (S'17) is currently pursuing Ph.D. degree in the Communications Engineering, CWC, UO.

Hirley Alves (S'11–M'15) is Associate Professor and Head of the Machine-type Wireless Communications Group at the 6G Flagship, CWC, UO.

Konstantin Mikhaylov (S'10-M'18-SM'19) is an Assistant Professor for Convergent IoT Communications for Vertical Systems with the CWC, UO.

Tong Hao (M'10) is currently a Professor at the College of Surveying and Geo-Informatics, Tongji University, Shanghai, China.